Acquisition Performance Comparison of the Generalized Maximum A Posteriori Symbol Synchronizer Versus the Data-Transition Tracking Loop

L. V. Lam,[1] T.-Y. Yan,[1] M. K. Simon,[1] and W. L. Martin[2]

A generalized maximum a posteriori (MAP) symbol synchronizer for arbitrary nonoverlapping pulse shape and data-transition density is derived, and a simplified realization is presented. Acquisition performance at low to very low symbol signal-to-noise ratios (SNRs) is investigated and compared against the conventional data-transition tracking loop (DTTL). Simulation results show that the MAP symbol synchronizer can operate at very low symbol SNRs where the DTTL fails. Furthermore, the new symbol synchronizer reduces the initial acquisition time by at least one order of magnitude as compared with the DTTL. It also has been shown that the new symbol synchronizer is suitable for minimum-shift-keying (MSK) signaling waveforms.

I. Introduction

Recent interest in employing powerful codes, such as turbo codes, for deep-space downlink communications motivates development of receivers operating at low symbol signal-to-noise ratios (SNRs), perhaps as low as -10 dB. At these values of symbol SNRs, traditional receivers using the data-transition tracking loop (DTTL) may experience difficulties in terms of symbol acquisition and tracking. The traditional DTTL is a suboptimal closed-loop implementation derived from the maximum a posteriori (MAP) estimation of the symbol epoch of a rectangular pulse stream in an additive white Gaussian noise (AWGN) environment.

A closed-loop symbol synchronizer, such as the DTTL, is obtained by using the first derivative of the log-likelihood function of the symbol epoch to approximate an error signal. When a rectangular pulse waveform is used, the derivative of the log-likelihood function does not exist; hence, strictly speaking, a closed-loop estimator does not exist for the rectangular pulse. Since the conventional DTTL approximates the first derivative of the rectangular pulse shape by a narrow pulse at its edges, it is pulse shape dependent. If a waveform other than the rectangular pulse is used for transmission, the conventional DTTL suffers a degradation during tracking and acquiring. Furthermore, the conventional DTTL was derived based on the assumption of a high SNR. Its performance will be degraded for low SNR applications [1].

[1] Communications Systems and Research Section.

[2] Future Missions Planning Office.

The generalized MAP symbol synchronizer described in this article is the optimal estimator for generating the time epochs. It received little attention in the past, mainly because it had been thought of as a "one-shot" estimator. The advent of powerful codes and the need to operate the receiver at low symbol SNRs, together with advances in digital signal-processing electronics, make this estimator an attractive choice for modern digital receiver implementations. In addition, it can be shown that the new symbol synchronizer not only can continuously update the estimate every symbol time, as does the closed-loop scheme, but also is less complex in implementation as compared with the conventional DTTL. This article quantifies the acquisition time performance of the MAP symbol synchronizer based on computer simulations. Several authors have presented performance bounds for the mean-square performance [2–6].[3] However, exact theoretical evaluation of the acquisition performance of the MAP estimator is mathematically difficult.

This article is organized into three sections. Section II derives the new symbol synchronizer for an arbitrary data-transition density. Section III presents computer simulation results for both the new estimator and the DTTL. Section IV provides the conclusion.

II. Theoretical Derivation

Consider the received baseband signal written in sample (discrete-time) form as

$$y(n) = \sqrt{S_T} \sum_k a_k p(n - kN - \varepsilon) + v(n) \tag{1}$$

where $n, k = 0, 1, \ldots, \infty, \varepsilon$ is the unknown symbol epoch, $p(n)$ is the nonoverlapping symbol pulse shape of duration T_s seconds, a_k is the kth binary symbol, N is the number of samples per symbol, S_T is the transmitted power, and $v(n)$ is the AWGN with a two-sided power spectral density level of $N_0/2$ W/Hz. Letting $\underline{y}_k$ denote the N-dimensional observation column vector of the signal in the kth symbol interval and $\underline{p}_k(\varepsilon), \underline{v}_k$ the corresponding nonoverlapping pulse shape and noise vectors, then

$$\underline{y}_k = \sqrt{S_T} a_k \underline{p}_k(\varepsilon) + \underline{v}_k \tag{2}$$

Letting $\underline{Y}_K$ be the observation vector over $K + 1$ symbols, then

$$\underline{Y}_K = \begin{bmatrix} \underline{y}_0 \\ \cdot \\ \cdot \\ \underline{y}_K \end{bmatrix} = \sqrt{S_T} \begin{bmatrix} a_0 \underline{p}_0(\varepsilon) \\ \cdot \\ \cdot \\ a_K \underline{p}_K(\varepsilon) \end{bmatrix} + \begin{bmatrix} \underline{v}_0 \\ \cdot \\ \cdot \\ \underline{v}_K \end{bmatrix} \tag{3}$$

Hence, the a posteriori probability density function of the symbol epoch, ε, given the received signal vector, $\underline{Y}_K$, is

$$P(\varepsilon|\underline{Y}_K) = \frac{P(\varepsilon)}{P(\underline{Y}_K)} \overline{P(\underline{Y}_K|\varepsilon, \underline{a}_K)}^{\underline{a}_K} \tag{4}$$

where the overline denotes statistical averaging over all possible values of the K-symbol data vector $\underline{a}_K$ and ε is assumed to be constant over K symbol intervals. Assuming an independent, identically

[3] M. K. Simon, "Maximum Likelihood Sliding Window Estimation of Timing for NRZ Data Streams," JPL Interoffice Memorandum (internal document), Jet Propulsion Laboratory, Pasadena, California, October 1997.

distributed (i.i.d.) data stream, $\underline{v}_K$ and $\underline{a}_K$ are uncorrelated, and $\underline{v}_K$ has zero mean and a variance of $N_0/2$ W/Hz. Then Eq. (3) can be rewritten as

$$P\left(\varepsilon|\underline{Y}_K\right) = \frac{P(\varepsilon)}{P\left(\underline{Y}_K\right)} \prod_{k=0}^{K} \sum_{a_k} P\left(\underline{y}_k|\varepsilon, a_k\right) P\left(a_k\right) \tag{5}$$

where $P(\underline{y}_k|\varepsilon, a_k)$ is conditionally Gaussian distributed as

$$P\left(\underline{y}_k|\varepsilon, a_k\right) = \frac{1}{\left(2\pi\frac{N_0}{2}\right)^{N/2}} \exp\left(-\frac{\left(\underline{y}_k - \sqrt{S_T}a_k\underline{p}_k(\varepsilon)\right)^T\left(\underline{y}_k - \sqrt{S_T}a_k\underline{p}_k(\varepsilon)\right)}{2\frac{N_0}{2}}\right) \tag{6}$$

where T denotes the transpose operation. For binary communication where a_k takes on values ± 1 and assuming ε is uniformly distributed over $\{0, 1, \ldots, N-1\}$, Eq. (5) can be reduced to

$$P\left(\varepsilon|\underline{Y}_K\right) = C\prod_{k=0}^{K}\left(2\alpha\sinh\left(2\frac{\sqrt{S_T}}{N_0}\underline{y}_k^T\underline{p}_k(\varepsilon)\right) + \exp\left(-2\frac{\sqrt{S_T}}{N_0}\underline{y}_k^T\underline{p}_k(\varepsilon)\right)\right) \tag{7}$$

where all the constant terms have been combined into C and α denotes the probability that $a_k = +1$. Since $P(\varepsilon|\underline{Y}_K)$ is a product of $K+1$ terms, it is easier to work with the logarithm of $P(\varepsilon|\underline{Y}_K)$. Taking the natural logarithm of Eq. (7) leads to the log-likelihood function

$$\Lambda\left(\varepsilon|\underline{Y}_K\right) = C_1 + \sum_{k=0}^{K}\ln\left(2\alpha\sinh\left(2\frac{\sqrt{S_T}}{N_0}\underline{y}_k^T\underline{p}_k(\varepsilon)\right) + \exp\left(-2\frac{\sqrt{S_T}}{N_0}\underline{y}_k^T\underline{p}_k(\varepsilon)\right)\right) \tag{8}$$

where $C_1 \equiv \ln(C)$. Since we are interested in maximizing $\Lambda(\varepsilon|\underline{Y}_K)$ with respect to ε, we can ignore the constant C_1. Letting $\alpha = 0.5$, Eq. (8) reduces to [1][4]

$$\Lambda\left(\varepsilon|\underline{Y}_K\right) = \sum_{k=0}^{K}\ln\left(\cosh\left(2\frac{\sqrt{S_T}}{N_0}\underline{y}_k^T\underline{p}_k(\varepsilon)\right)\right) \tag{9}$$

The generalized MAP estimate of the epoch is the estimate, $\hat{\varepsilon}$, which maximizes the log-likelihood function of Eq. (9). That is,

$$\Lambda\left(\hat{\varepsilon}|\underline{Y}_K\right) = \max_{i=0,1,\ldots,N-1}\left\{\Lambda\left(\varepsilon_i|\underline{Y}_K\right)\right\} \tag{10}$$

where

$$\varepsilon_i \in \{0, 1, \ldots, N-1\} \tag{11}$$

[4] Ibid.

The argument in Eq. (9) can now be rewritten as the discrete convolution

$$\underline{y}_k^T \underline{p}_k(\varepsilon_i) = \sum_{n=(k-1)N+i}^{kN+i-1} y(n)p(n-(k-1)N) \tag{12}$$

Hence, Eqs. (9) and (12) specify a realization of the generalized MAP symbol synchronizer. It involves discretely correlating the symbol pulse waveform with all possible shifted received signals. Equation (9) can be rewritten in the recursive form:

$$\Lambda\left(\varepsilon|\underline{Y}_K\right) = \Lambda\left(\varepsilon|\underline{Y}_{K-1}\right) + \ln\left(\cosh\left(2\frac{\sqrt{S_T}}{N_0}\underline{y}_K^T\underline{p}_K(\varepsilon)\right)\right) \tag{13}$$

From Eqs. (12) and (13), a recursive implementation of the MAP symbol synchronizer is realized and shown in Fig. 1 [1].[5]

For practical implementation, one can simplify the estimator, as shown in Fig. 2, where the coefficients of the finite impulse response (FIR) filter correspond to N samples of the digitized symbol pulse waveform. The look-up table performs the operation shown in Figs. 1(b) or 1(c). Resetting the accumulator can be accomplished by the preprogram clock with period K or by using the reset signal generator circuitry shown in Fig. 2(b). Note that it is difficult to determine the appropriate value of period K when the symbol SNR is not known. The circuit shown in Fig. 2(b) automatically provides the reset timing needed to reset the accumulator.

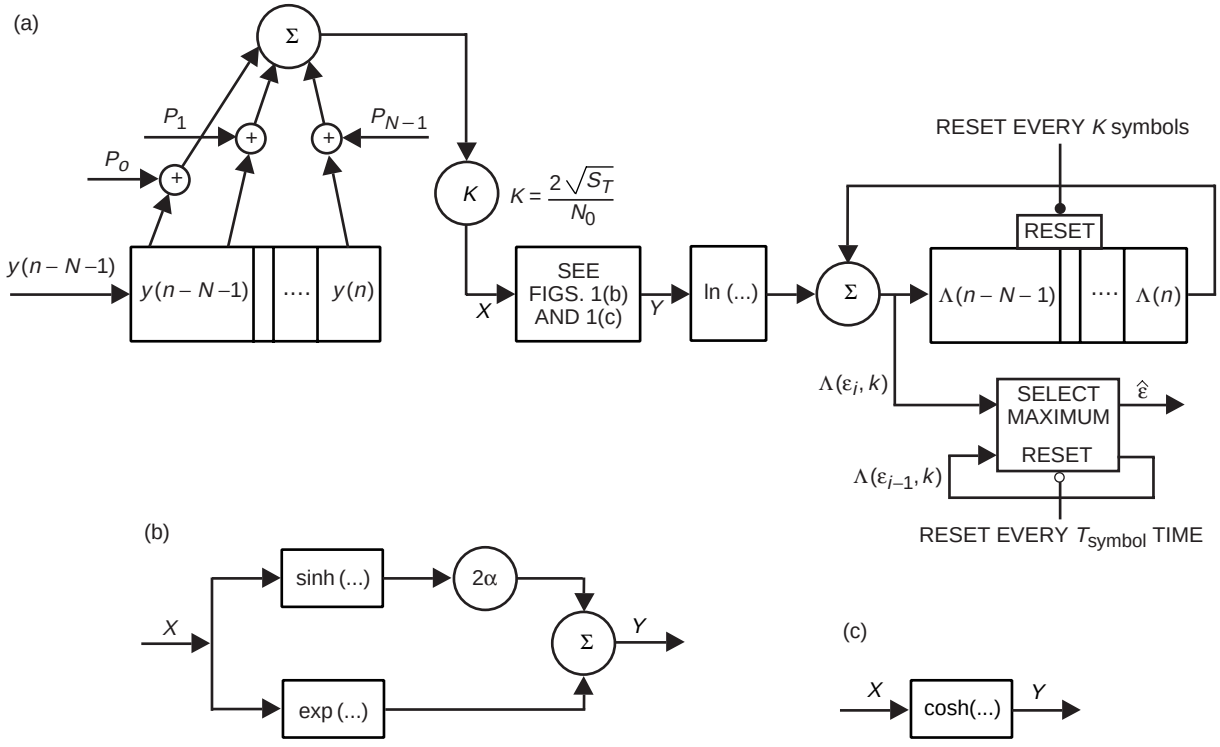

Fig. 1. The recursive MAP symbol synchronizer: (a) implementation, (b) implementation when the probability of mark (α) ≠ 0.5, and (c) implementation when the probability of mark = 0.5.

[5] Ibid.

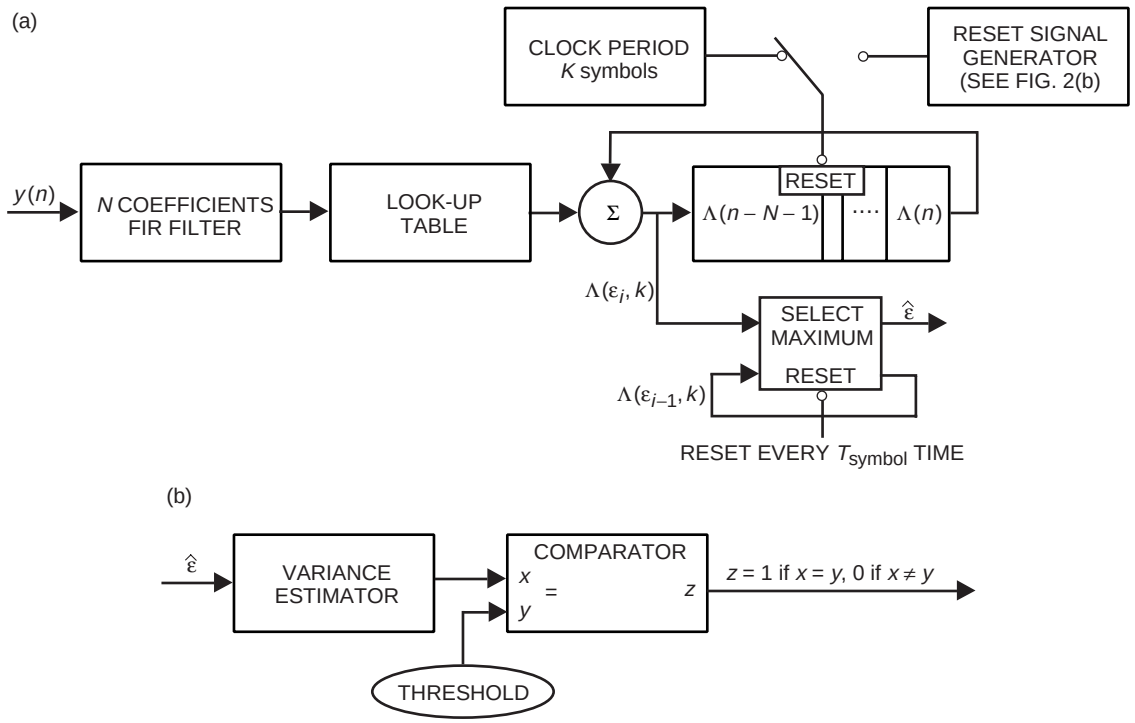

Fig. 2. The simplified estimator: (a) the simplified recursive MAP symbol synchronizer and (b) the reset signal generator.

III. Computer Simulation

Figure 3 shows the communication simulation system in order to compare the acquisition performance of the two symbol synchronizers using the Signal Processing Worksystem (SPW) software from Cadence Design Systems. Table 1 summarizes the simulation parameters.

A. Acquisition Performance of the MAP Symbol Synchronizer

Figure 4(a) shows the probability of acquisition as a function of acquisition time parameterized by the symbol SNR. Each acquisition curve is obtained from 500 simulation runs. For each run, a random epoch is chosen for the symbol synchronizer to acquire. The epoch is assumed to be uniformly distributed over the discrete symbol interval $\{0, 1, \ldots, N-1\}$. The MAP symbol-synchronizer acquisition time is the time at which the synchronizer declares lock and the normalized error between the estimate and the actual epoch is equal to or less than a prescribed value for at least 5 seconds. The normalized error is defined as

$$\lambda = \frac{|\varepsilon - \hat{\varepsilon}_k|}{T_s} \tag{14}$$

where $\hat{\varepsilon}_K$ is the estimate of the symbol epoch made after observing K data symbols. Note that $\hat{\varepsilon}_K$ is discrete, with values in the range of $(0, 1, \ldots, N-1)$, while the unknown symbol epoch, ε, is continuous. Hence, when ε is not an integer multiple of $1/N$, the estimate, $\hat{\varepsilon}_K$, will have an irreducible error component of magnitude $|\Delta| < 1/N$. The error component is inversely proportional to the sampling frequency: the higher the sampling frequency (larger N), the smaller the error component, Δ. In this article, ε always is an integer multiple of Δ.

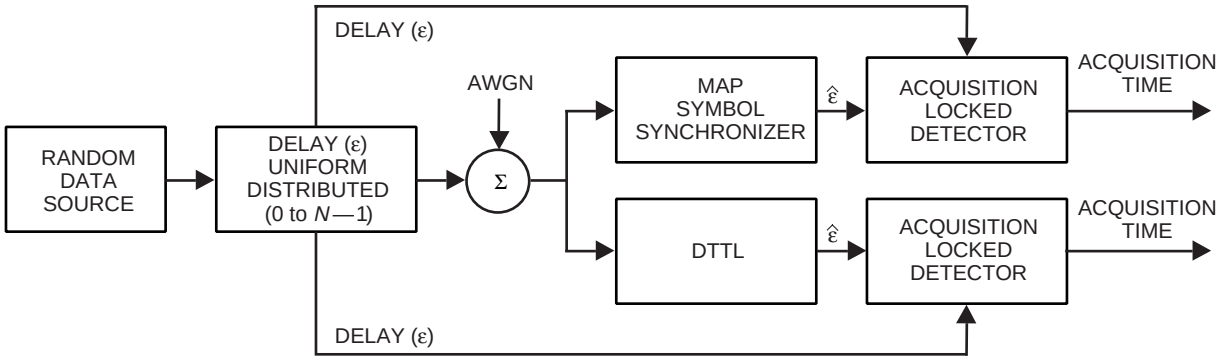

Fig. 3. The computer simulation model for evaluating the acquisition performance of the MAP symbol synchronizer and the DTTL.

Table 1. Simulation parameters.

Parameter	Value
Sampling frequency, f_s	500 kHz
Symbol rate, R_s	10 kHz
No. samples/symbol, N	50

Figure 4(a) shows the probability of acquisition curves when the prescribed value of the normalized error, λ, is set to less than Δ. Figure 4(b) shows the probability of acquisition curves with the normalized error, λ, set to less than Δ and 2Δ. As expected, the acquisition time decreases because larger errors can be tolerated. Note that λ is a function of the variable N.

It often is practical to have small N to minimize processing power and hardware complexity. Reducing N means increasing the irreducible error component Δ. However, the estimate could reach the steady state in a shorter period of time. Figure 4(c) shows the probability of acquisition as a function of acquisition time for various values of N. Here the normalized error, λ, is set to less than Δ, and ε is an integer multiple of Δ.

The MAP estimator shown in Fig. 1 can accommodate data unbalance (i.e., a data-transition density not equal to 0.5). Figure 1(b) shows the implementation for arbitrary α, and Fig. 1(c) shows the case for $\alpha = 0.5$. Since α is not known a priori, Fig. 1(c) represents a suboptimal implementation when α is unequal to 0.5. Figure 5 shows the probability of acquisition versus acquisition time curves for $\alpha = 0.7$. The solid curves result from using the nonlinearity in Fig. 1(b), and the dashed curves result from using the nonlinearity shown in Fig. 1(c). Note that using the correct nonlinearity [i.e., Fig. 1(b)] improves the acquisition probability, but not significantly. The following simulations will not consider transition unbalance in the data probabilities.

The generalized MAP symbol synchronizer shown in Fig. 1 is applicable to any symbol pulse shape, provided that the coefficients of the FIR filter contain the samples of the pulse shape waveform. In this experiment, the half-sinusoidal waveform of the minimum-shift-keying (MSK) signaling was digitized into 50 samples ($N = 50$) and chosen as the FIR filter coefficients. Figure 6(a) shows the probability of acquisition as a function of time for the MSK waveform. Note that $\lambda < 2\Delta$ is used in Fig. 6(a).

Although the generalized MAP symbol synchronizer was designed for nonoverlapping pulse shapes [i.e., zero intersymbol interference (ISI)], simulation results show that it does work with overlapping

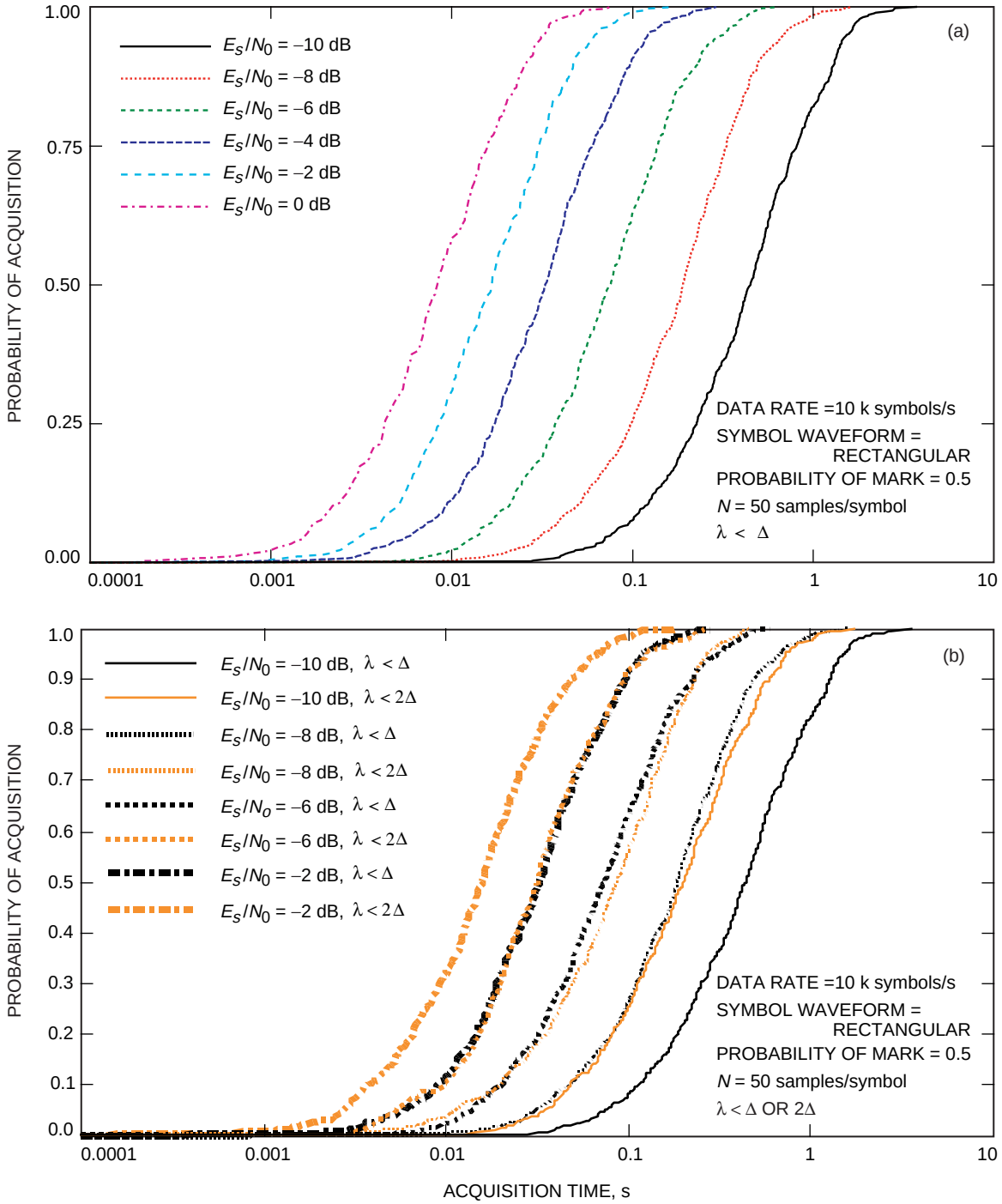

Fig. 4. The acquisition performance of the MAP symbol synchronizer parameterized by: (a) the symbol SNR, (b) the symbol SNR and normalized estimation error, λ, and (c) the number of samples/symbol, *N*.

pulse shapes that produce ISI. Figure 6(b) shows the probability of acquisition versus acquisition time for a Gaussian-minimum-shift-keying (GMSK) pulse shape with a Gaussian filter bandwidth-to-bit time product ($BT_B = 0.25$). Note that in order for the generalized MAP symbol synchronizer to work properly with ISI pulses, one must allow sufficiently large values of λ to discount the effects of ISI.

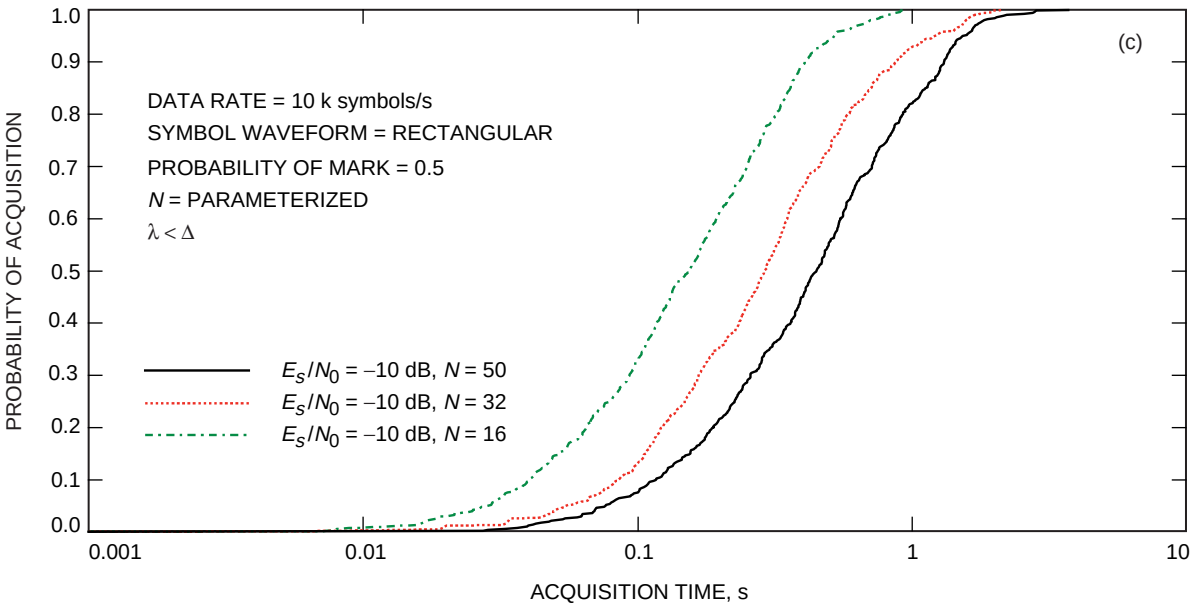

Fig. 4 (cont'd). The acquisition performance of the MAP symbol synchronizer parameterized by: (a) the symbol SNR, (b) the symbol SNR and normalized estimation error, λ, and (c) the number of samples/symbol, *N*.

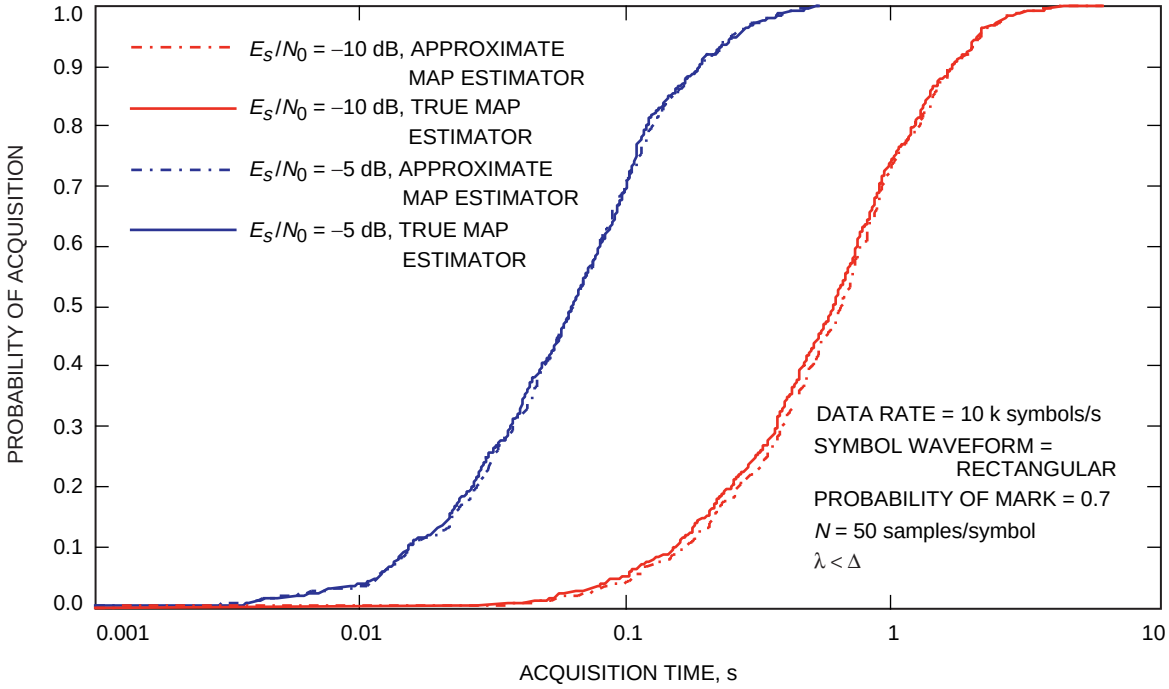

Fig. 5. The acquisition performance of the MAP symbol synchronizer for the approximate and true MAP estimators.

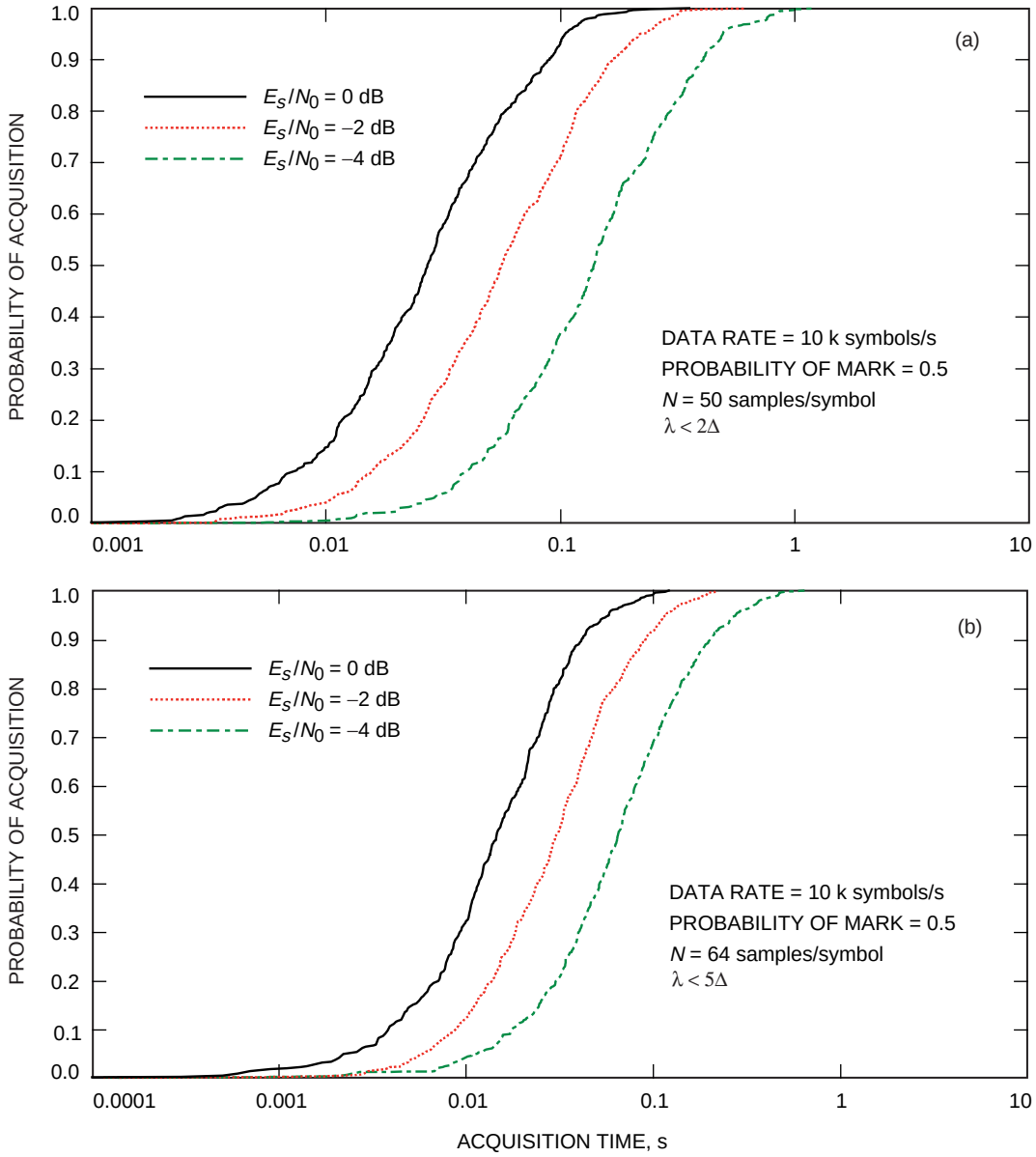

Fig. 6. The acquisition performance of the MAP symbol synchronizer for (a) an MSK waveform and (b) a GMSK (BT_B = 0.25) waveform.

B. Acquisition Performance of the DTTL Tracking Loop

The acquisition and tracking performance of the DTTL has been studied extensively[6] [1,7–9] at medium-to-high symbol SNRs. Since the DTTL was developed for this SNR range, one would expect sub-optimal performance for low symbol SNR applications. Figure 7(a) shows the probability of acquisition as a function of time for the DTTL at various symbol SNRs.

Similarly to those described in Section II.A, each probability of acquisition curve was generated from 500 simulation runs. Acquisition is declared when the phase error (λ_{DTTL}) stays less than or equal to a

[6] H. Tsou and S. Hinedi, "SPW Simulation for Clock Stability Effects on Acquisition Performance of the Data Transition Tracking Loop," CCSDS Action Item A-E-93-37 (internal document), Jet Propulsion Laboratory, Pasadena, California, June 1994.

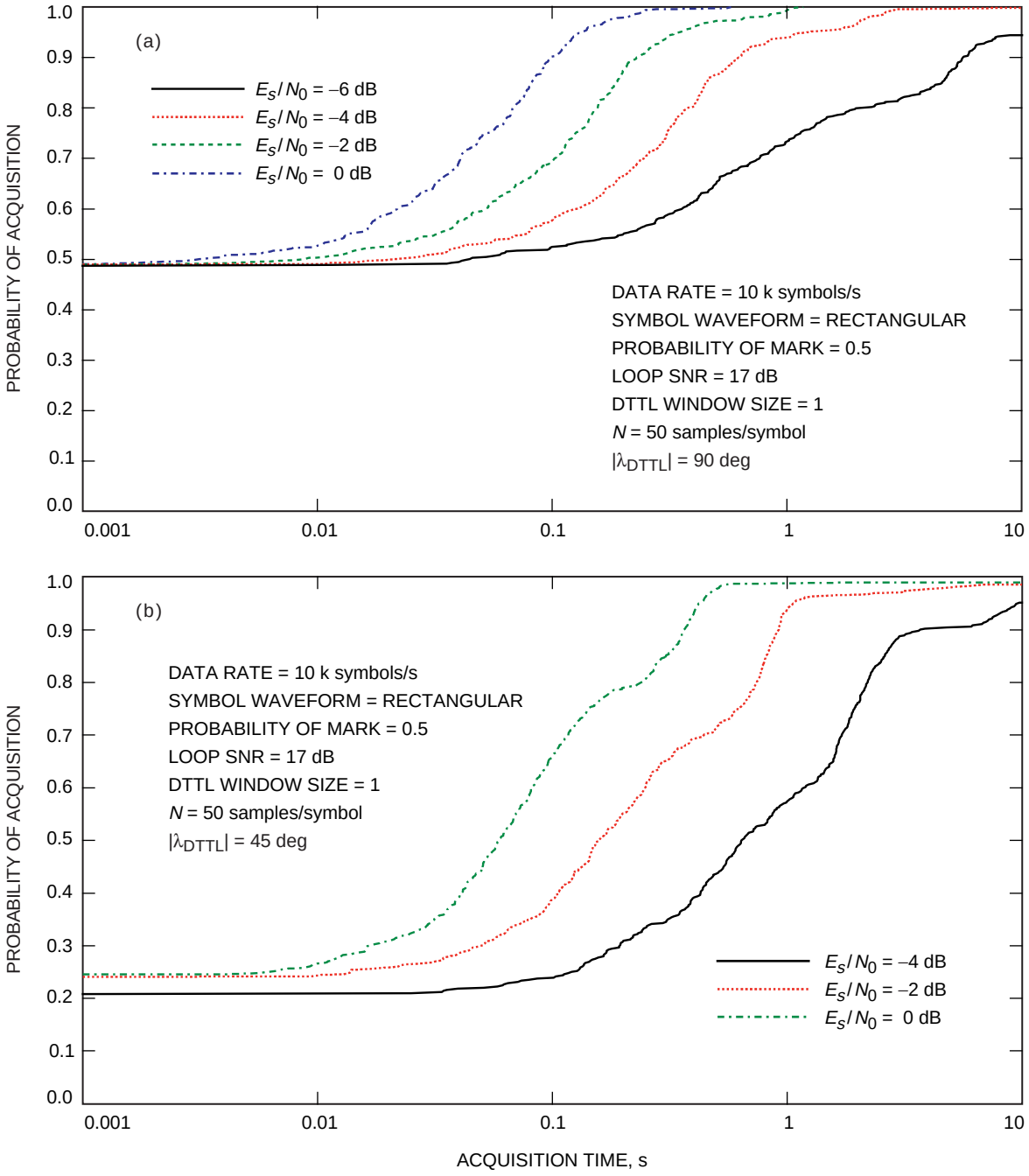

Fig. 7. The acquisition performance of the DTTL parameterized by symbol SNR with: (a) loop SNR = 17 dB and prescribed phase error = 90 deg, (b) loop SNR = 17 dB and prescribed phase error = 45 deg, and (c) loop SNR = 10 dB and prescribed phase error = 90 deg.

prescribed value for at least $10/B_L$ seconds, where B_L is the DTTL's loop filter bandwidth. With the loop SNR set to 17 dB, the normalized window size = 1 (full window), and the prescribed phase error set to 90 deg (the pull-in range of the DTTL), Fig. 7(a) shows the probability of acquisition versus acquisition time. Note that these curves show that the acquisition performance of the DTTL degrades significantly as symbol SNR becomes smaller. At symbol SNRs below −5 dB, the DTTL sometimes fails to acquire within the allotted time. For example, at a symbol SNR = −6 dB, the DTTL failed to acquire after 418 seconds in some simulations. The probability of acquisition curves for symbol SNRs below −6 dB are

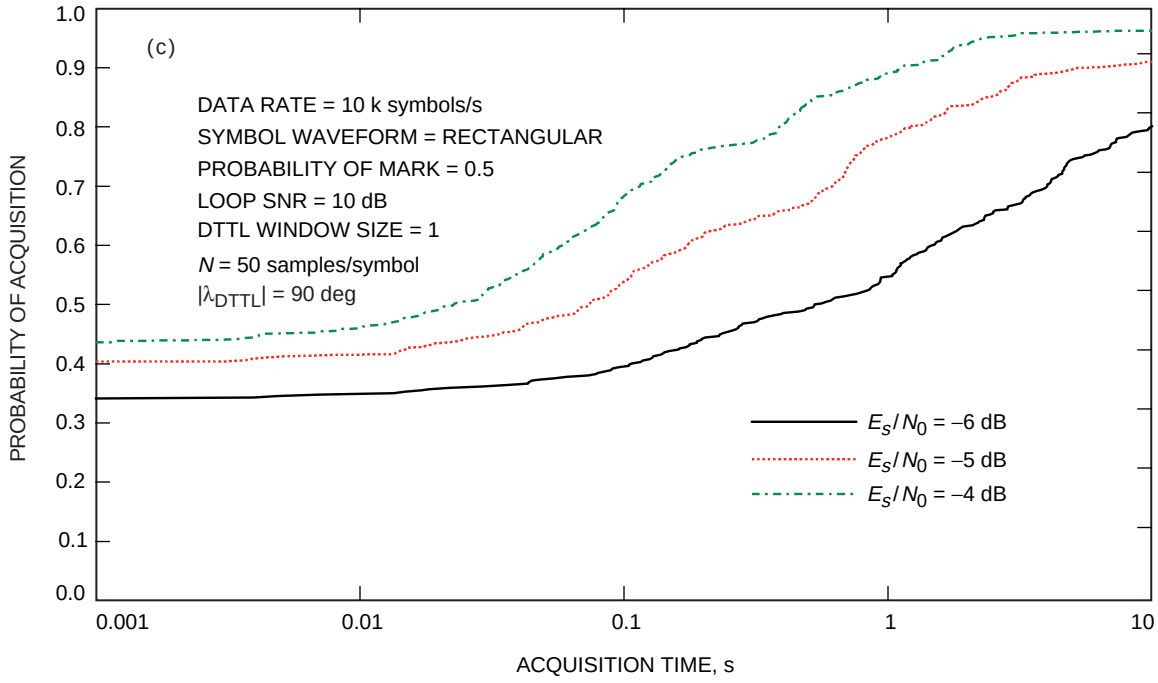

Fig. 7 (con't). The acquisition performance of the DTTL parameterized by symbol SNR with: (a) loop SNR = 17 dB and prescribed phase error = 90 deg, (b) loop SNR = 17 dB and prescribed phase error = 45 deg, and (c) loop SNR = 10 dB and prescribed phase error = 90 deg.

not available, due mainly to the fact that, in this range of SNRs, either the DTTL often does not lock or it would take an extremely long time to generate one of these curves even if the DTTL could acquire at these low SNRs. In Fig. 7(b), the acquisition probability curves were obtained with the prescribed phase error reduced to 45 deg.

Acquisition time of the DTTL is a function of the bandwidth of the loop filter and the window size. Aung et al. [9] have discussed the optimization of these parameters. Increasing the loop bandwidth (i.e., decreasing the loop SNR) is equivalent to increasing the update rate; hence, the acquisition time *could* become smaller. However, increasing the loop bandwidth also means increasing the noise power in the loop; hence, the loop could become unstable, especially at low symbol SNRs. Figure 7(c) shows the acquisition probability curves as a result of widening the bandwidth of the loop filter (i.e., decreasing the loop SNR from 17 dB down to 10 dB). Comparing Fig. 7(a) with Fig. 7(c) shows that the acquisition performance becomes worse for lower loop SNRs (i.e., for larger bandwidths of the loop filter).

C. A Comparison of the Acquisition Performance of the MAP Symbol Synchronizer and the DTTL

A comparison of Figs. 4(a) and 4(b) with Figs. 7(a) and 7(b) clearly shows the advantages of the new symbol synchronizer compared with the DTTL in terms of acquisition time. For a given probability of acquisition, the new symbol synchronizer provides faster acquisition time even under a more stringent criterion, namely smaller phase error. Note that the new symbol synchronizer can acquire, with 100 percent probability, a signal with an SNR as low as −10 dB, provided that the symbol epoch remains unchanged. This was not true for the DTTL. Figure 8 summarizes the performance difference between the new symbol synchronizer and the DTTL by showing the acquisition time as a function of symbol SNR for an acquisition probability of 90 percent. Acquisition time of the new symbol synchronizer (Fig. 8) ranges from a 10-dB improvement at symbol SNRs less than −5 dB to a 3-dB improvement for a symbol SNR about 0 dB, when compared with the DTTL. Note that it is not surprising to see that the acquisition time of the new symbol synchronizer decreases linearly with increasing symbol SNR, as shown in Fig. 8

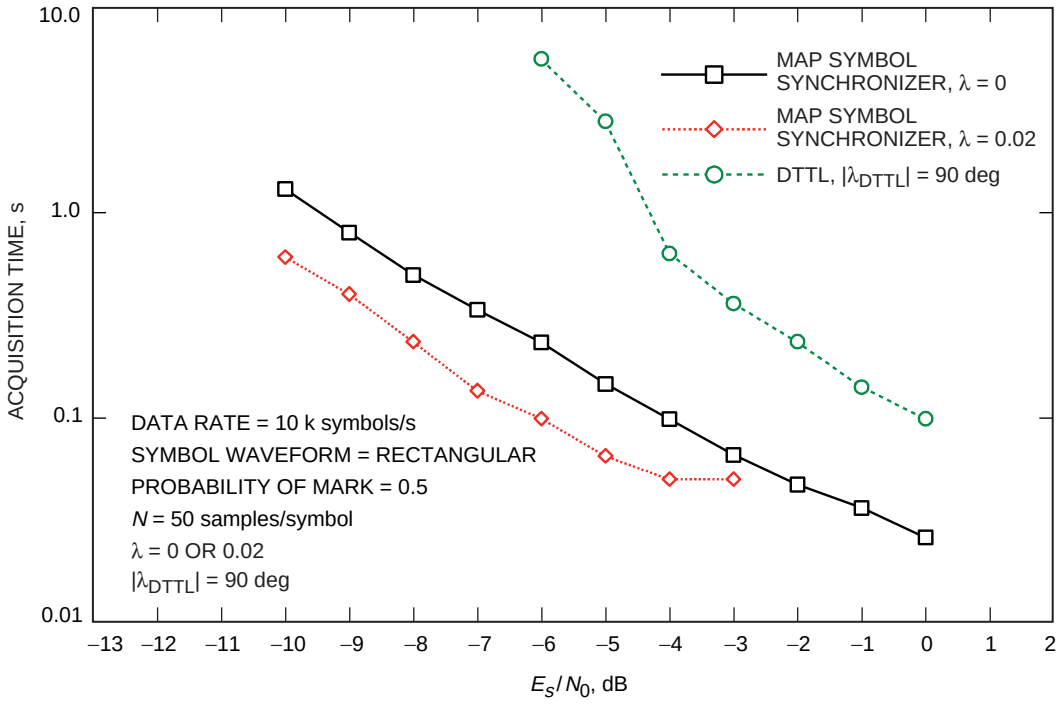

Fig. 8. The acquisition time as a function of symbol SNR for a probability of acquisition = 0.9.

($\lambda < \Delta$). For the AWGN channel, the noise power decreases linearly as a function of the observation time. Hence, increasing the symbol SNR linearly is equivalent to decreasing the observation time linearly (i.e., shortening the acquisition time).

IV. Conclusion

In this article, the generalized MAP symbol synchronizer for arbitrary data-transition density was derived and, based on computer simulation, shown to provide orders of magnitude improvement over the conventional DTTL in terms of acquisition time, particularly at low symbol SNRs. In addition, with the recursive implementation, the MAP symbol synchronizer can continuously update (at the symbol rate) the estimate, as shown in Fig. 1. For example, as shown in Figs. 4 through 6, at symbol SNR = −10 dB, one can update the estimate at least once every 4 seconds with a 90 percent probability that the new estimate has zero tracking phase error. The DTTL will take an order of magnitude longer, provided that it can acquire at a symbol SNR of −10 dB with reasonable phase error.

References

[1] W. C. Lindsey and M. K. Simon, *Telecommunication Systems Engineering*, Chapter 9, Englewood Cliffs, New Jersey: Prentice-Hall, 1973.

[2] J. Ziv and M. Zakai, "Some Lower Bounds on Signal Parameter Estimation," *IEEE Trans. on Inform. Theory*, vol. IT-15, pp. 386–391, May 1969.

[3] D. Chasan, M. Zakai, and I. Ziv., "Improved Lower Bounds on Signal Parameter Estimation," *IEEE Trans. on Inform. Theory*, vol. IT-21, pp. 90–93, January 1975.

[4] I. Ibragimov and R. Khas'minskii, "Parameter Estimation for a Discontinuous Signal in White Gaussian Noise," *Problemy Peredachi Informatsii*, vol. 11, no. 3, pp. 31–43, July–September 1975, as translated in *Problems of Information Transmission*, pp. 203–212, September 1976.

[5] A. Terent'yev, "Distribution of the Time of Absolute Maximum at the Output of a Matched Filter," *Radio Engineering and Electronic Physics*, vol. 13, no. 4, pp. 569–573, 1968.

[6] K. Kosbar, *Open and Closed Loop Delay Estimation with Applications to Pseudonoise Code Tracking*, Ph.D. Dissertation, University of Southern California, Los Angeles, California, July 1988.

[7] C.-S. Tsang and C. M. Chie, "Effect of Signal Transition Variation on Bit Synchronizer Performance," *IEEE Trans. on Communications*, vol. COM-41, no. 5, pp. 673–677, May 1993.

[8] S. Million and S. M. Hinedi, "Effects of Symbol Transition Density on Tracking and Acquisition Performance of the Data Transition Tracking Loop at Low Signal-to-Noise Ratios," *The Telecommunications and Data Acquisition Progress Report 42-128, October–December 1996*, Jet Propulsion Laboratory, Pasadena, California, pp. 1–9, February 15, 1997.
http://tda.jpl.nasa.gov/tda/progress_report/42-128/128A.pdf

[9] M. Aung, W. J. Hurd, C. M. Buu, J. B. Berner, S. A. Stephens, and J. M. Gevargiz, "The Block V Receiver Fast Acquisition Algorithm for the Galileo S-Band Mission," *The Telecommunications and Data Acquisition Progress Report 42-118, April–June 1994*, Jet Propulsion Laboratory, Pasadena, California, pp. 83–114, August 15, 1994.
http://tda.jpl.nasa.gov/tda/progress_report/42-118/118I.pdf